Journal of
Nanoscience and Nanotechnology
Vol. 13, 8106–8109, 2013

RESEARCH ARTICLE

Formation of Gallium Vacancies and Their Effects on the Nanostructure of Pd/Ir/Au Ohmic Contact to *p*-Type GaN

Kyong Nam Kim[1], Tae Hyung Kim[1], Jin Seok Seo[1], Ki Seok Kim[1], Jeong Woon Bae[1], and Geun Young Yeom[1, 2, *]

[1] *Department of Advanced Materials Science and Engineering, Sungkyunkwan University, Suwon, 440-746, Korea*
[2] *Sungkyun Advanced Institute of Nanotechnology (SAINT), Suwon, 440-746, Korea*

The properties of Pd/Ir/Au ohmic metallization on *p*-type GaN have been investigated. Contacts annealed at 400 °C in O_2 atmosphere demonstrated excellent ohmic characteristics with a specific contact resistivity of 1.5×10^{-5} Ω-cm^2. This is attributed to the formation of Ga vacancies at the contact metal-semiconductor interfacial region due to the out-diffusion of Ga atoms. The out-diffusion of Ga atoms was confirmed by X-ray photoelectron spectroscopy depth profiles, high-resolution transmission electron microscopy, and electron energy loss spectroscopy using a scanning transmission electron microscope.

Keywords: *p*-Type Contact, GaN, LED, Ohmic Contact, Pd, Ir, Au.

1. INTRODUCTION

Ohmic contact formation on GaN-based materials is one of the critical steps in the fabrication of high performance, short wavelength, light emitting diodes (LEDs) and laser diodes. Various metallization schemes, along with surface preparation methods, metal deposition techniques, and annealing processes have been investigated to improve the performance of *p*-type GaN contacts.[1–5] However, forming excellent ohmic contacts on *p*-type GaN has been a challenge because the work function of *p*-GaN is as high as 6.7 eV.[6] This high work function is too large for any metal to form a barrier-free metal-semiconductor junction with *p*-GaN without inducing a significant material reaction or introducing a high hole more than high 10^{18} cm^{-3} near the *p*-GaN surface.

The most useful strategy for overcoming the high work function of *p*-GaN is to cause a moderate reaction between the contact metals and *p*-GaN. This reaction induces the formation of gallium vacancies below the contacts, which act as acceptors, and they lead to high near-surface carrier concentrations. To date, researchers[7–10] have used X-ray photoelectron spectroscopy (XPS) and Auger electron spectroscopy (AES) to demonstrate the formation of Ga vacancies and the out-diffusion of Ga atoms from *p*-GaN. XPS data provide information on atomic composition and atomic binding states. In addition, the data they provide information on the shifts in the Fermi energy level for the detection of changes in the semiconductor work function. However, other microanalysis methods are required to conclusively support the out-diffusion of gallium vacancies toward the contact materials.

We propose high-resolution transmission electron microscopy (HRTEM) and electron energy loss spectroscopy (EELS) using a scanning transmission electron microscope (STEM) for profile mapping of the atomic Ga at the metal-semiconductor interface to directly determine the formation of Ga vacancies. Especially, in this study, Pd/Ir/Au metallization is used to form a low resistance ohmic contact to *p*-type GaN. To understand the mechanism of the ohmic contact formation, we investigated (1) the carrier transport process across the metal/*p*-type GaN interface using current–voltage–temperature (I–V–T) measurements, (2) depth profiles of Ga atoms in the metal/*p*-GaN interfacial region using XPS, and (3) atomic depth profiles of Ga atoms at the metal/*p*-type GaN interface using HRTEM and EELS.

2. EXPERIMENTAL DETAILS

The sample used in this work consisted of a 1 μm-thick Mg-doped GaN layer grown at 970 °C at 300 Torr by

*Author to whom correspondence should be addressed.

 1533-4880/2013/13/8106/004 doi:10.1166/jnn.2013.8192

metal-organic chemical vapor deposition (MOCVD) on a GaN buffer layer grown at 1045 °C on a (0001) sapphire substrate. Trimethylgallium (TMGa), NH_3, and biscyclopentadienyl (Cp_2Mg) were used as source materials of Ga, N, and *p*-type dopants, respectively. Holes were electrically activated by annealing the sample in N_2 atmosphere for 5 min at 1000 °C. Carrier concentration after the activation process was determined to be $\sim 4.5 \times 10^{17}$ cm^{-3} by Hall measurement. Contact metals consisting of Pd (10 nm)/Ir (10 nm)/Au (30 nm) were deposited by electron beam evaporation at deposition rate of 6 nm/min. Samples were annealed in O_2 atmosphere at 400 °C or 500 °C in a rapid thermal annealing system.

Specific contact resistivities were calculated using a linear transmission line model (L-TLM).[9] The I–V–T characteristics of the contacts were measured using a four-point-probe at temperatures ranging from −50 to 150 °C. HRTEM and EELS were performed in a JEOL 2010F STEM system to investigate the formation of Ga vacancies and the interdiffusion of contact and semiconductor materials.

3. RESULTS AND DISCUSSION

Electrical measurements conducted at room temperature confirmed the ohmic behavior of the Pd/Ir/Au contacts on the *p*-type GaN annealed at 400 °C (sample #S1) and 500 °C (sample #S2). The best ohmic behavior was obtained at 400 °C with a specific contact resistivity (ρ_c) of as low as 1.5×10^{-5} Ω-cm^2. The temperature-dependent ρ_c values of contacts #S1 (square) and S2 (circle) from the current–voltage–temperature (I–V–T) measurements are shown in Figure 1. Also shown is the theoretical value of ρ_c (solid line) of the contacts to *p*-GaN as a function of measurement temperature. Calculations were performed for the case where the carrier transport mechanism is dominated by field emission (FE). The theoretical curve was obtained from the following equations,[11–13]

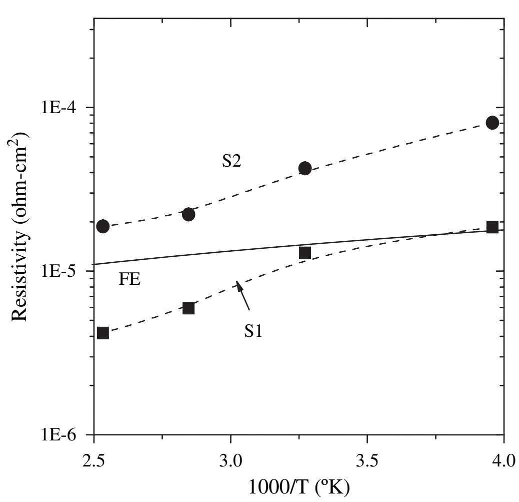

Fig. 1. Theoretical (solid line) and experimental (symbols with dotted lines) temperature-dependent specific contact resistivities as a function of $1/T$ for the samples S1 (square) annealed at 400 °C and S2 (circle) annealed at 500 °C.

$$\rho_C \approx (k/qA^{**}T) * \exp(q\Phi_B/E_{oo}) \quad \text{for } FE,\ E_{oo}/kT >> 1 \quad (1)$$

where,

$$E_{oo} = qh/4\pi[N_a/m^* e_s]^{1/2} = 1.86 \times 10^{-11}[N_a/m^* e_s]^{1/2}\ \text{(ev)} \quad (2)$$

E_{oo} is a characteristic energy related to the tunneling probability, N_a is the hole carrier concentration, m^* is the effective mass, e_s is the permittivity of *p*-GaN, q is the elementary charge, k is the Boltzman constant, Φ_B is the barrier height, A^{**} is the Richardson constant, h is the Plank's constant, and T is the absolute temperature. The Richardson constant, A^{**}, was set to $4\pi q k^2 m^*/h^3 = 120(m^*/m)$ = 96 A/cm^2 K^2. In Figure 1, the experimental curve of the temperature-dependent ρ_c of the contact (#S1) shows good agreement with the theoretical curve at temperatures below 300 °K, while the gap between the experimental and theoretical curves increases as the temperature increases, indicating that thermionic emission (TE) also affects the transport process. The FE transport behavior can be attributed to an increment in the net hole concentration caused by the formation of Ga vacancies below the contact interface. Typically, the transition from thermionic-field emission (TFE) to FE occurs at doping concentrations over 10^{18}/cm^3.[13–15] And, the concentration of the samples used in this study after the activation process was 5×10^{17} cm^{-3}.

In order to demonstrate the formation of Ga vacancies at the interface between Pd/Ir/Au and *p*-GaN, narrow-scan spectroscopy was carried out several times. Detailed information on the interface region for S1 was obtained using XPS. For a facility For simplicity, the metal thickness was set to Pd/Ir/Au = 5/5/15 nm. *In-situ* sputter thinning was carried out at a low sputter rate of 1 nm/min for the contact metals. All of metal peaks completely disappeared after 36 min of sputter thinning. Narrow scan XPS spectra corresponding to the Ga 2*p* core level for different scan depths are shown in Figure 2. The peak at 1115.9 eV, assigned to the Ga in the Ga—N bond at the surface region of GaN, (curve *a*), shifted toward a higher binding energy as the sputtering depth approached the bulk *p*-type GaN, (curve *e*), where we assumed *e* no Ga vacancies. The binding energy shift is due to a change in the Fermi energy level, which is caused by the formation of Ga vacancies due to the out-diffusion of Ga atoms.[7,9,10] The production of Ga vacancies in the near-surface region of GaN should lead to an increase in the net hole concentration just below the contact, resulting in a decrease of the depletion region width. Consequently, more carriers can tunnel through the

RESEARCH ARTICLE

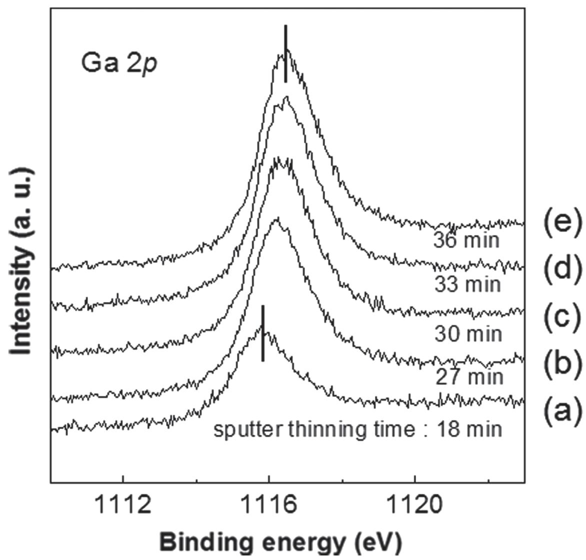

Fig. 2. Narrow scan XPS spectra of Ga2*p* core level peaks for the contact annealed at 400 °C (S1).

reduced effective barrier at the metal/semiconductor interface region.

To further investigate the formation of Ga vacancies, we analyzed the interdiffusion behavior between the contact materials and Ga atoms at the interface region using HRTEM combined with EELS in a STEM. HRTEM images of the metal/*p*-GaN interfacial region of the contact annealed at 400 °C are shown in Figure 3. The width of the reaction region between the metal and GaN could be observed in the figure. In order to quantify the Ga distribution across the interface region, EELS was performed on the samples that were imaged with HRTEM. The < 1 nm diameter electron probe in the STEM scanned across the interface region proceeding from the GaN into the metal as shown in Figure 4(a). Several scans were performed and the Ga signal was monitored. Data were acquired in the line-spectrum mode with energy dispersion of 0.5 eV/channel. The electron probe size was less than 1 nm and the distance between two successive probe positions was 0.8 nm. Quantitative analysis of Ga was carried out by using the signal extracted from the Ga 2*p* edge corresponding to the L_2 and L_3 peaks. The two-dimensional map of the Ga distribution obtained using EELS is shown in Figure 4(b). The reaction region was determined to be 16 nm. From Figure 4(b), it can be seen that a small amount of Ga diffused out toward the metal contact material to produce a shallow Ga vacancy layer just below the reaction region.

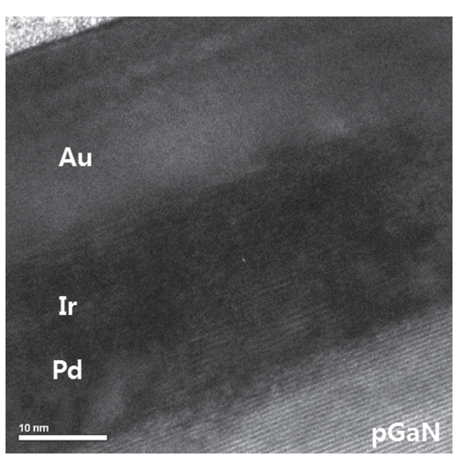

Fig. 3. HRTEM images for the Pd/Ir/Au contact annealed at 400 °C.

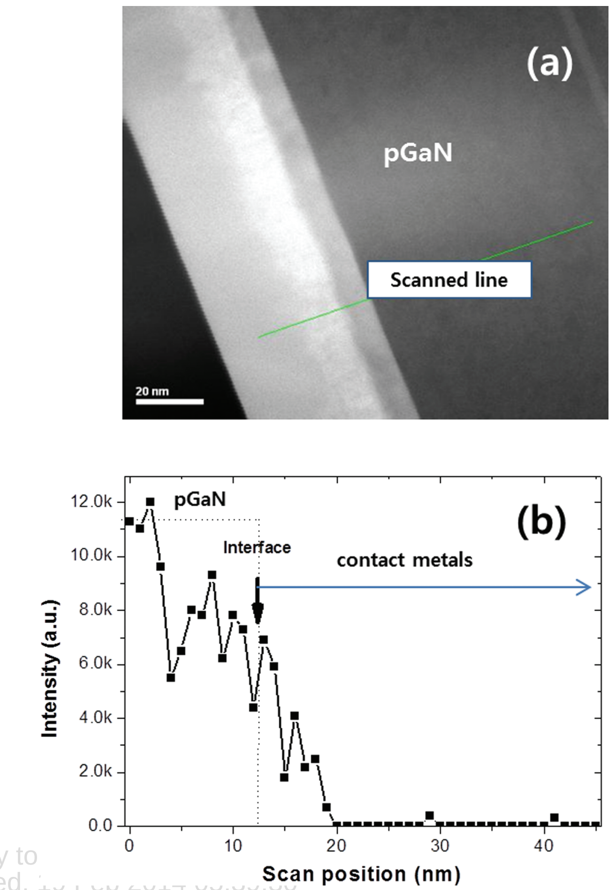

Fig. 4. Cross section image of Pd/Ir/Au contact to GaN by STEM (a) and two-dimensional map of the Ga distribution obtained using an EELS line-spectrum (b).

4. CONCLUSION

The Pd/Ir/Au contact scheme on *p*-type GaN exhibited ohmic behavior with a specific contact resistivity as low as 1.5×10^{-5} Ω-cm^2 at the annealing temperature of 400 °C. The out-diffusion of Ga was shown by a combination of XPS, HRTEM, and EELS. The contact formation mechanism resulting in the low specific contact resistivity was attributed to the formation of Ga vacancies, which acted as deep acceptors below the contacts; thus the carrier concentrationwas increased and the effective Schottky barrier height was reduced overall.

Acknowledgments: This work was supported by the Industrial Strategic technology development program (10041926, Development of high density plasma technologies for thin film deposition of nanoscale semiconductor and flexible display processing) funded by the Ministry of Knowledge Economy (MKE, Korea) and Nano Material Technology Development Program through the National Research Foundation of Korea (NRF) funded by the Ministry of Education, Science and Technology (2012M3A7B4035323).

References and Notes

1. T. Maeda, Y. Koide, and M. Murakami, *Appl. Phys. Lett.* 75, 4145 (**1999**).
2. L. Zhou, W. Lanford, A. T. Ping, J. W. Yang, A. Khan, and I. Adesida, *Appl. Phys. Lett.* 76, 3451 (**1999**).
3. V. Advarahan, A. Lunev, M. Asif Khan, J. Yang, G. Simin, M. S. Shur, and R. Gaska, *Appl. Phys. Lett.* 78, 2781 (**2001**).
4. H. S. Oh, S. M. Kim, J. H. Joo, J. H. Baek, and J. S. Kwak, *J. Nanosci. Nanotechnol.* 11, 1503 (**2011**).
5. H. S. Lee, H. W. Shin, and S. B. Jung, *J. Nanosci. Nanotechnol*. 12, 3210 (**2012**).
6. R. J. Nemanich, M. C. Benjamin, S. W. King, M. D. Bremser, R. F. Davis, B. Chen, Z. Zhang, and J. Bernholc, Gallium nitride and related materials, *Mater. Res. Soc. Symp. Proc.*, edited by R. D. Dupuis, J. A. Edmond, F. A. Ponce, and S. Nakamura, Pittsburgh, PA (**1996**), Vol. 395.
7. H. K. Kim, T.-Y. Seong, I. Adesida, C. W. Tang, and K. M. Lau, *Appl. Phys. Lett.* 84, 1710 (**2004**).
8. B. H. Jun, H. Hirayama, and Y. Aoyagi, *Jpn. J. Appl. Phys.* 41, 581 (**2002**).
9. J. O. Song, D.-S. Leem, J. S. Kwak, O. H. Nam, Y. Park, and T.-Y. Seong, *Appl. Phys. Lett.* 83, 2372 (**2003**).
10. J. O. Song, D.-S. Leem, and T.-Y. Seong, *Appl. Phys. Lett.* 83, 3513 (**2003**).
11. K. Varahramyan and E. J. Verret, *Solid-State Electronics* 39, 1601 (**1996**).
12. J.-S. Jang and T.-Y. Seong, *Appl. Phys. Lett.* 76, 2743 (**2003**).
13. A. Y. C. Yu, *Solid-State Electron.* 13, 239 (**1970**).
14. J. I. Pankove, S. Bloom, and G. Harbeke, *RCA Rev.* 36, 163 (**1975**).
15. C. R. Crowell and V. L. Rideout, *Solid-State Electron.* 12, 89 (**1969**).

Received: 6 January 2013. Accepted: 14 May 2013.